Available online at www.sciencedirect.com
ScienceDirect
Carbohydrate Polymers 73 (2008) 427–437
Carbohydrate Polymers
www.elsevier.com/locate/carbpol

# Preparation and characterization of konjac glucomannan/poly(diallydimethylammonium chloride) antibacterial blend films

Jun Lu [a,c], Xiaodan Wang [b], Chaobo Xiao [a,*]

[a] College of Chemistry and Molecular Sciences, Wuhan University, Wuhan 430072, People's Republic of China
[b] College of Life Sciences, Wuhan University, Wuhan 430072, People's Republic of China
[c] Department of Chemistry and Bioscience, Xiangfan University, Xiangfan 441003, People's Republic of China

Received 19 September 2007; received in revised form 28 November 2007; accepted 13 December 2007
Available online 31 December 2007

**Abstract**

A novel antibacterial film was prepared by blending konjac glucomannan (KGM) and poly(diallydimethylammonium chloride) (PDADMAC) in an aqueous system. The antibacterial activity of the films against *Staphylococcus aureus*, *Bacillus subtilis*, *Escherichia coli*, *Pseudomonas aeruginosa*, and *Saccharomyces* were measured by the halo zone test and the double plate method. The films exhibited an excellent antibacterial activity against *B. subtilis* and *S. aureus* but not against *E. coli*, *P. aeruginosa* or *Saccharomyces*. The miscibility, morphology, thermal stability, water vapour permeability and mechanical properties of the blend films were investigated by density determination, SEM, ATR-IR, XRD, DSC, TGA, WVA and tensile tests. The results of density determination predicted that the blends of KGM and PDADMAC were miscible when the PDADMAC content was less than 70 wt%. Moreover, SEM and XRD confirmed the result. ATR-IR showed that strong intermolecular hydrogen bonds and electrostatic interactions occurred between KGM and PDADMAC in the blends. The tensile strength and the break elongation of the blends were improved largely to 106.5 MPa and 32.04% and the water vapour permeability decreased when the PDADMAC content was 20 wt%. The thermal stability of the blends was higher than pure KGM. The blends should be good antibacterial materials.
© 2007 Elsevier Ltd. All rights reserved.

*Keywords:* KGM; PDADMAC; Blending; Performance; Antibacterial

## 1. Introduction

Growing concerns regarding the safety of food warrant a greater emphasis on the development of active packaging. To prevent the development and spread of pathogenic microorganisms via food, more information is needed concerning potential alternatives such as antibacterial packaging materials (MollLler, Grelier, Pardon, & Coma, 2004). According to Cooksey (2005), there are three basic categories of antimicrobial films. One involves the direct incorporation of the antimicrobial additive into the packaging film. The second type is coated with a material that acts as a carrier for the additive. However, legal issues and standards concerning the rate of migration of substances in packaging into food products limit the development of such bioactive materials (Coma et al., 2002; Begin & Van Calsteren, 1999). Thirdly, antimicrobial macromolecules with film-forming properties, such as chitosan, can produce antimicrobial films. But the greatest obstacle to the development of chitosan-based packaging is cost (Li, Kennedy, Peng, Yie, & Xie, 2006).

Among natural polymers, konjac glucomannan (KGM) is a good candidate for packaging materials. It has attracted great interest since had excellent film-forming ability, good biocompatibility and biodegradability. KGM, one of the a high molecular weight water-soluble non-ionic natural poly-

* Corresponding author. Tel.: +87 27 87210143.
*E-mail address:* CBXiao@whu.edu.cn (C. Xiao).

0144-8617/$ - see front matter © 2007 Elsevier Ltd. All rights reserved.
doi:10.1016/j.carbpol.2007.12.021

saccharide found in tubers of the *Amorphophallus konjac*, is composed of β-(1→4)linked D-glucose and D-mannose in the molar ratio of 1:1.6 with a low degree of acetyl groups (Nishinari, Williams, & Phillips, 1992). It has wide applications in food (Cheng, Abd Karim, Norziah, & Seow, 2002; Chun, Kim, & Yoo, 2006; Li, Peng, Yie, & Xie, 2006) and biomedical (Cuna et al., 2006; Alvarez-Mancenido et al., 2006; Alonso-Sande, Cuna, & Remunan-Lopez, 2006; Chen, Liu, & Zhuo, 2005; Yu, Huang, & Xiao, 2006) domains. Although a good film-forming material candidate for food and fruit preservation, KGM has the common flaws of natural polymers, low mechanical properties and poor antimicrobial activity. In our early work, we found that blending is a convenient and effective method to improve the physicochemical properties and function of the films (Xiao, Gao, Wang, & Zhang, 2000). Therefore we selected poly(diallydimethylammonium chloride) (PDADMAC) as the partner with KGM and investigated the physicochemical and antibacterial properties of KGM/ PDADMAC (KP) films.

PDADMAC, the first synthetic polymer to be approved by the U.S. Food and Drug Administration for the use in potable water treatment possesses a backbone of cyclic units and highly hydrophilic permanently charged quaternary ammonium groups. It is safe for human health and has wide uses in paper manufacturing, water treatment industry, mining industry and biological, medical and food processes (Wandrey, Hernandez-Barajas, & Hunkeler, 1999). It is a strong cationic polyelectrolytes with antibacterial properties, however, it is not a good film-forming material and is highly hygroscopic. We predict that a gland would be a better forming material better than either KGM or PDADMAC alone.

In this study, the antibacterial activity of these film blends against *Staphylococcus aureus*, *Bacillus subtilis*, *Escherichia coli*, *Pseudomonas fluorescens* and *Saccharomyces* were measured by the halo zone test and the double plate method. Furthermore the miscibility, morphology, thermal stability, Water vapour permeability and mechanical properties of the blend films were investigated by density determination, scanning electron microscopy (SEM), attenuated total reflection infrared spectroscopy (ATR-IR), X-ray diffraction (XRD), differential scanning calorimetry (DSC), thermo-gravimetric analysis (TGA), WVA and tensile tests. We believe that this work may contribute basic information to the further application of KGM and PDADMAC in packaging films and biomedical materials.

## 2. Experimental

### 2.1. Materials

KGM powder (purity 99%) was purchased from Huaxianzi Konjac Co. Ltd. (Hubei, China) and was used without further purification. The viscosity is 10 Pa s in 1 wt% concentration. DADMAC (65 wt% solution in water) monomer were supplied by Wuhan Jiangrun Fine Chemical Co. Ltd.; Ammonium peroxydisulfate (APS), sodium thiosulfate pentahydrate (STP) and ethylene diamine-tetraacetic acid disodium salt (EDTA) were purchased from Shantou Xilong Chemical Factory (Guangdong,China). All other chemicals were reagent grade and used without further purification.

The test strains, *S. aureus* Rosenbach, *B. subtilis* 168, *E. coli* HB101, *Pseudomonas fluorescens* AB92001, and *Saccharomyces cerevisiae*, used for this study were provided by the collection Center of Wuhan University.

### 2.2. Synthesis and characterization of PDADMAC

PDADMAC was prepared by radical polymerization according to the following method: DADMAC were polymerized at 60 °C for 5 h under a $N_2$ atmosphere, by using APS/STP as initiator and EDTA as accelerator. The ratios of APS/DADMAC, STP/ DADMAC and EDTA/DADMAC were 0.02/1, 0.015/1 and 0.008/1(W/W). The resulting viscous solution was poured into an open beaker containing methanol/acetone (v/v 1:5). The white solid polymer, PDADMAC was deposited and poured into the glass plate, then dried under vacuum at 40 °C until constant weight, stored in desiccators. In order to confirm the polymerization, the $^1$H NMR spectra of DMDAAC and PDMDAAC were recorded on a Varian Mercury-VX-300 spectrometer at 300 MHz, chemical shifts in ppm were relative to $Me_4Si$. The intrinsic viscosity ($[\eta]$) of PDADMAC was 123.7 mL g$^{-1}$, determined by an Ubbelohde capillary viscometer (Chinese Academy of Sciences, China) at 25 ± 0.1 °C, using 0.5 M NaCl as solvent. According to the Mark-Houwink equation $[\eta] = 1.12 \times 10^{-4} M_v^{0.82}$ (Wandrey, Jaeger, & Reinisch, 1982), the viscosity-average molecular weight ($M_v$) of PDADMAC was 5142.

### 2.3. Preparation of the KP films

The KGM/PDADMAC ratios were 100/0, 90/10, 80/20, 70/30, 60/40, 50/50, 40/60, 30/70, 0/100(W/W), relative to dry KGM, with a total mass of 1.0 g. The PDADMAC and KGM were dissolved in 20 and 80 mL distilled water, respectively and stirred vigorously to form a uniform solution. The mixture was stirred vigorously at 25 °C for 1 h and degassed. Finally, it was poured on to glass plates and water evaporated at room temperature for 2 days. The films of different ratios above were coded as KP0, KP1, KP2, KP3, KP4, KP5, KP6, KP7 and KP10, respectively. Since the blend films containing more than 70 wt% PDADMAC formed two phases to the naked eyes obviously and had little mechanical strength, they were discarded.

### 2.4. Characterization of the KP films

The densities ($\rho$) of the KP films were determined using the equilibrium sedimentation method (Kirker & Prestwich, 2004), which required the use of two miscible liquids in which the polymer sample did not dissolve or swell. It was also required that the sample float in one liquid and

sink in the other. The KP film was placed in a glass vial with 3.0 mL of tetrachloride. Next, absolute ethanol was added dropwise until the sample began to sink. The dropwise addition of ethanol continued until the sample was suspended in solution, at which time the density of the solution was taken to be equal to the density of the KP sample. The density was determined by weighing 1.0 mL of solution. The average density was calculated from three separate density determinations.

Scanning electron microscopy (SEM) images of the films were taken with a microscope (JEOL 6700 F, Japan). The films were cut into pieces and snapped, and then vacuum-dried. The surface and cross-section of the films were sputtered with gold, and then observed and photographed.

X-ray diffraction (XRD) patterns were recorded on an X-ray diffraction instrument (XRD-6000 Shimadzu, Japan), by using $CuK_\alpha$ radiation ($\lambda = 0.1542$ nm) at 40 kV and 30 mA with a scan rate of 4°/min. The diffraction angle ranged from 10° to 50°.

IR spectra of the films were recorded using a Fourier transform infrared (FTIR) spectrometer (Nicolet 170SX, USA) with attenuated total reflection instruments for investigation intermolecular interaction. The films were taken on the flat sheet and data were collected over 64 scans with a resolution of 4 $cm^{-1}$ at room temperature.

DSC was performed using a Netzsch DSC 200 PC at a heating rate of 10 °C/min under nitrogen atmosphere. The temperature ranged from 20 to 500 °C.

Thermal gravimetric measurements were performed using Netzsch STA 449C instrument (Germany) under a nitrogen atmosphere with a flow capacity of 30 mL/min. The scan was carried out at a heating rate of 10 °C/min from 20 to 500 °C. The sample weight was about 8–10 mg and analyzed using $\alpha$-$Al_2O_3$ crucible.

Tensile strength ($\sigma_b$) and elongation ($\varepsilon_b$) at break of the films were measured on a versatile electron tensile tester (CMT-6503, Shenzhen SANS Test Machine Co. Ltd., China) with a tensile rate of 5 mm/min. The size of the films strips was 70 × 10 × 50 mm (length × width × distance between two clamps). The mean values of $\sigma_b$ and $\varepsilon_b$ were obtained from five replications, respectively.

Water vapour permeability (WVP) tests were conducted following ASTM (1989) method E96–80. The test film was sealed as a patch onto a glass permeation cell containing silica gel (RVP = 0) with a 1.5 cm-deep headspace. The cell was then placed in a desiccator maintained at 25 °C and RVP = 0.22 using a saturated salt solution of potassium acetate. The cell was weighed daily over a 7-day period. Changes in weight of the cell were plotted as a function of time. The constant rate of weight gain was obtained by linear regression with $r^2 \geqslant 0.99$. The water vapour transmission rate (WVTR) was calculated from the slope of the straight line divided by the test area ($A$). WVP (kg $Pa^{-1}$ $s^{-1}$ $m^{-1}$) was calculated as $WVP = [WVTR/S(R_1 - R_2)] \times d$, where $S$ is saturation vapor pressure (Pa) of water at test temperature, $R_1$ is RVP in the desiccator, $R_2$ is RVP in the permeation cell, and $d$ is film thickness (m).

### 2.5. Antimicrobial assay

Antimicrobial activity tests of the films were carried out using the halo zone test and the double plate method. The test strains were *S. aureus*, *B. subtilis*, *E. coli*, *P. fluorescens* and *Saccharomyces*. Fifteen microliters of 50 mg/mL solutions of the films were added to the filter paper discs. The filter paper discs were placed on the agar plates, which had been previously seeded with 0.1 ml of inoculum containing indicator microorganisms in the range of 100 CFU/ml. The plates with *S. aureus*, *B. subtilis*, *E. coli* were then incubated at 37 °C for 24 h, the plates with Pseudomonas and Saccharomyces were incubated at 28 °C for 24 h. The diameters of inhibitory zones surrounding the filter paper discs were observed. The double plate method shows the detailed antibacterial activity of the blends. Firstly 100 μL of the bacterial solution was spread on the LB plate and dried for 3 h. Then 100 uL of 10 mg/mL antibacterial materials covered the plate and cultured. The plates were then photographed.

## 3. Results and discussion

### 3.1. Characterization of PDADMAC

As shown in Fig. 1, PDADMAC is a linear polymer with a backbone of cyclic units and charged quaternary ammonium groups and can be obtained by the cyclopolymerization of DADMAC. NMR spectroscopy was used to confirm the polymerization. The $^1H$ NMR spectra of DMDAAC and PDMDAAC are shown in Fig. 2. As for the spectra of the monomer, the methyl protons of N—$CH_3$ gave a single resonance peak at 2.83 ppm; the doublet peaks at 3.70 and 3.72 ppm were assigned to the methylene protons of N—$CH_2$; the triplet peaks at 5.53 and 5.85 ppm were attributed to the olefin protons of the —CH= and $CH_2$= respectively. The results are in agreement with a previous report (Yang et al., 2003). Compared to the monomer, the triplet peaks of the olefin protons disappeared in the spectra of the polymer, which indicated that polymerization occurred. In addition, methyl protons of N—$CH_3$ gave the double peaks at 2.95 and 3.06 ppm; the multiplet resonance peaks at 3.41 and 3.64 ppm were assigned to the protons of N—$CH_2$ and —CH— because of coupling each other; the peaks at 1.00 ppm corresponded to methylene

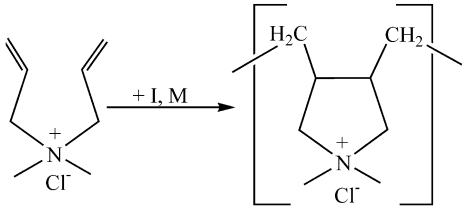


Fig. 1. Cyclopolymerization of DADMAC and the structure of PDADMAC.

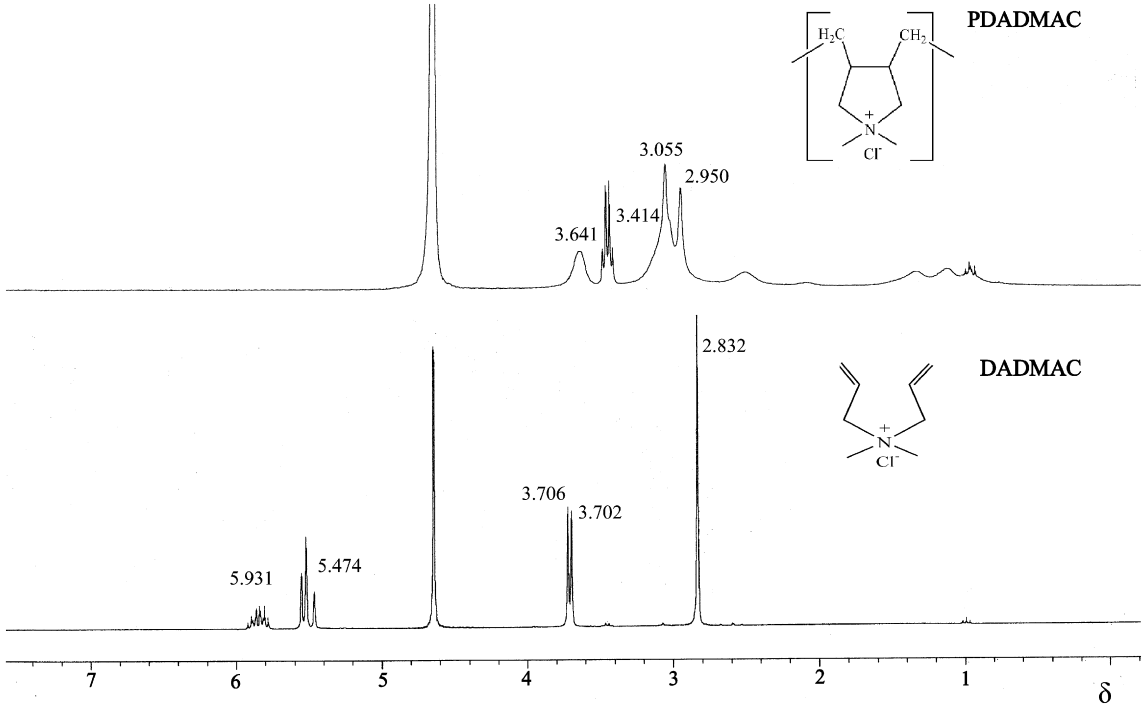


Fig. 2. $^{1}$H NMR spectra of the DMDAAC monomer and polymer.

protons unbonded with quaternary nitrogen. All the changes were attributed to the ring polymerization.

### 3.2. Miscibility between KGM and PDADMAC in the blend films

Usually, in a polymer blend, where there is no adhesion between the polymer interface and no molecular mixing at the phase boundary, the densities of the blend would be expected to follow the additivity rule of mixtures (Kim, Klempner, & Frisch, 1976). The variations in the densities of the KP films as a function of the PDADMAC content were depicted graphically as shown in Fig. 3. When the PDADMAC content was less than 70 wt%, the experiment density values of the KP films were obviously higher than that calculated theoretically, suggesting a strong adhesion existence between KGM and PDADMAC. The result could be explained if the PDADMAC molecules penetrated into the KGM leading to a reduction of the free volume of the film blends. Therefore, the films possessed higher densities than that of pure KGM and PDADMAC. It could be predicted that PDADMAC and KGM have good miscibility in the blends when the PDADMAC content was less than 70 wt%. The SEM images of the blends would confirm the result directly.

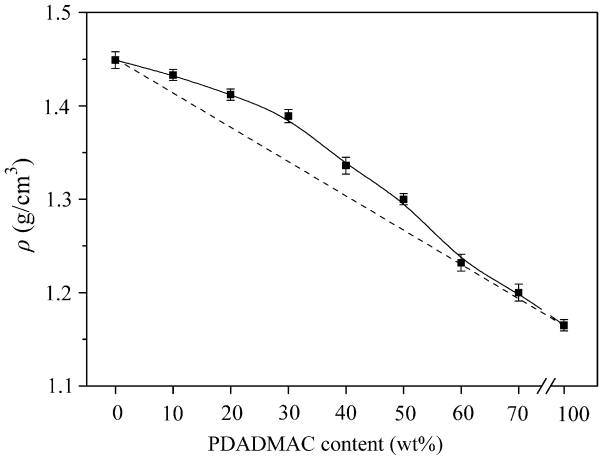


Fig. 3. Dependence of the density on the PDADMAC content for the KP films ("---", the dash line was expressed to the theoretical density of the KP films).

### 3.3. Morphology of the films

Fig. 4 shows the SEM images of the surfaces for the films KP2, KP5, KP7 and KP10. The image of KP10, the pure functional polymer PDADMAC, showed a regular crystal morphology, with a radiated flower-like pattern. From the image of KP7, it was found that the shape of the surface morphology changed from this pattern to ordered lines, but were still homogeneous and smooth. As to the image of KP5, most of the morphology was homogeneous and there were some assemble particles in the homogeneous matrix. As to KP2, a homogeneous morphology was displayed and the assemble particles became small and uniform. It can be seen that as the KGM content increased, the morphology of the blend film surfaces changed from smooth to microphase separation, implying that the two polymers had good miscibility, which may have

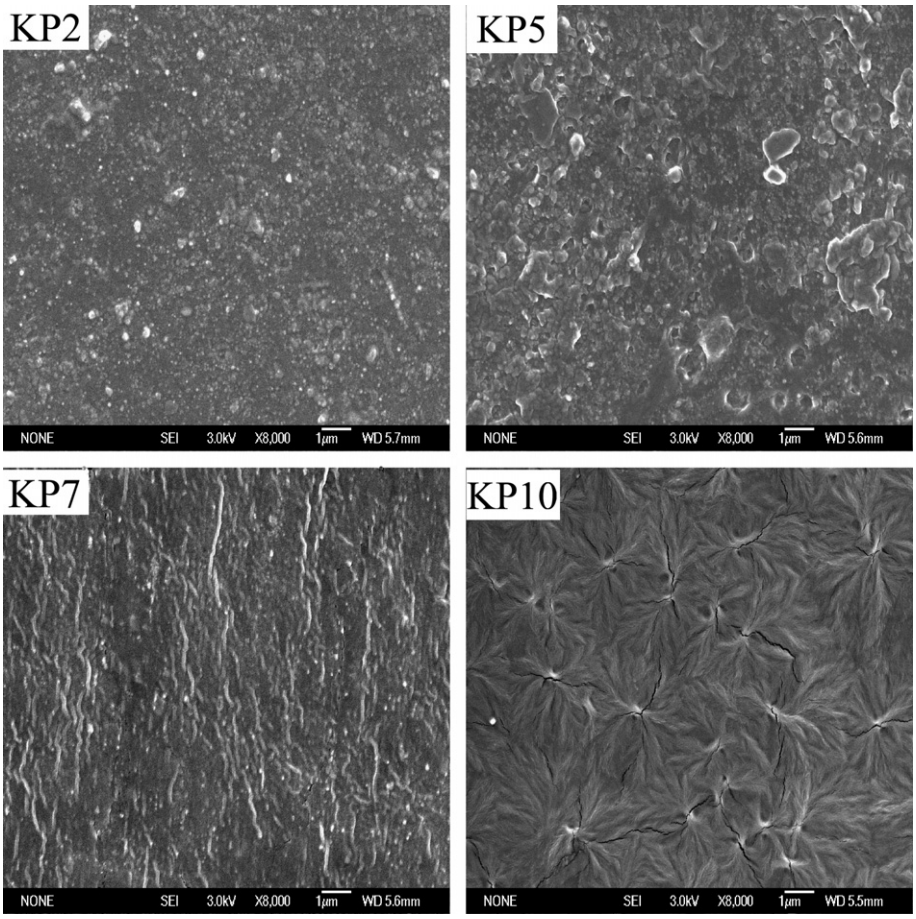


Fig. 4. SEM images of the surfaces of the KP films.

led to the decrease in crystallinity (Yang, Zhang, & Feng, 1999). It was very interesting that all of the blends had a homogeneous morphology, but different microstructures were displayed. Both the natural and synthetic polymers were water-soluble, so it was not surprising that a homogeneous morphology was observed. Therefore it can be concluded that there exist interactions between the two polymers, which resulted the different miscibility and microstructure of the blends. The highest miscibility occurred when the PDADMAC content was 20 wt%. However, the intermolecular interaction restrained the crystal behavior of PDADMAC with the increasing of KGM content, so different microstructures were obtained. The nature of the interaction between the two polymers, will be discussed later.

Fig. 5 shows the SEM images of the cross-sections of the films. All of the films displayed uniform and dense morphology. However the morphology changed from smooth to rough with the increasing PDADMAC content. Therefore it can be predicted that PDADMAC and KGM had good miscibility in the blend films, but the microstructure of the blends was affected by the PDADMAC content.

XRD was used to probe the crystal behavior of the blends. X-ray diffraction patterns of the KP blend films are shown in Fig. 6. The pattern of KGM showed a broad peak at $2\theta = 21.3°$, and several small and weak peaks appeared at 14.40°, 37.85° and 44.08°. The pattern of PDADMAC showed a broad peak and a stronger peak at $2\theta = 16.39°$, 22.04°, 27.57° and 31.92°, respectively. If KGM and the other polymer had low compatibility, each polymer would have its own crystal region in the blend films, X-ray diffraction patterns would be expressed simply as mixed patterns of KGM and the other polymer with the same ratio as those for blending (Xiao, Lu, Gao, & Zhang, 2001). Fortunately, the case did not occur in the blend films. Comparing the patterns of KP2, KP5 and KP7 to that of KP10, it was obvious that the diffraction peak at 16.39°, 22.04°, 27.57° and 31.92° became weaker with the reduction of PDADMAC down to 20 wt% and hardly appeared finally. It can be expected that the intermolecular interactions between KGM and PDADMAC made the PDADMAC molecules disperseinto the KGM matrix and the crystal behavior of PDADMAC was restrained. Consequently, the crystalinity of PDADMAC decreased and good blend miscibility resulted. The result supported the SEM conclusion that good miscibility existed between KGM and PDADMAC when the PDADMAC content was less than 70 wt% and the highest miscibility appeared when the PDADMAC content was 20 wt%.

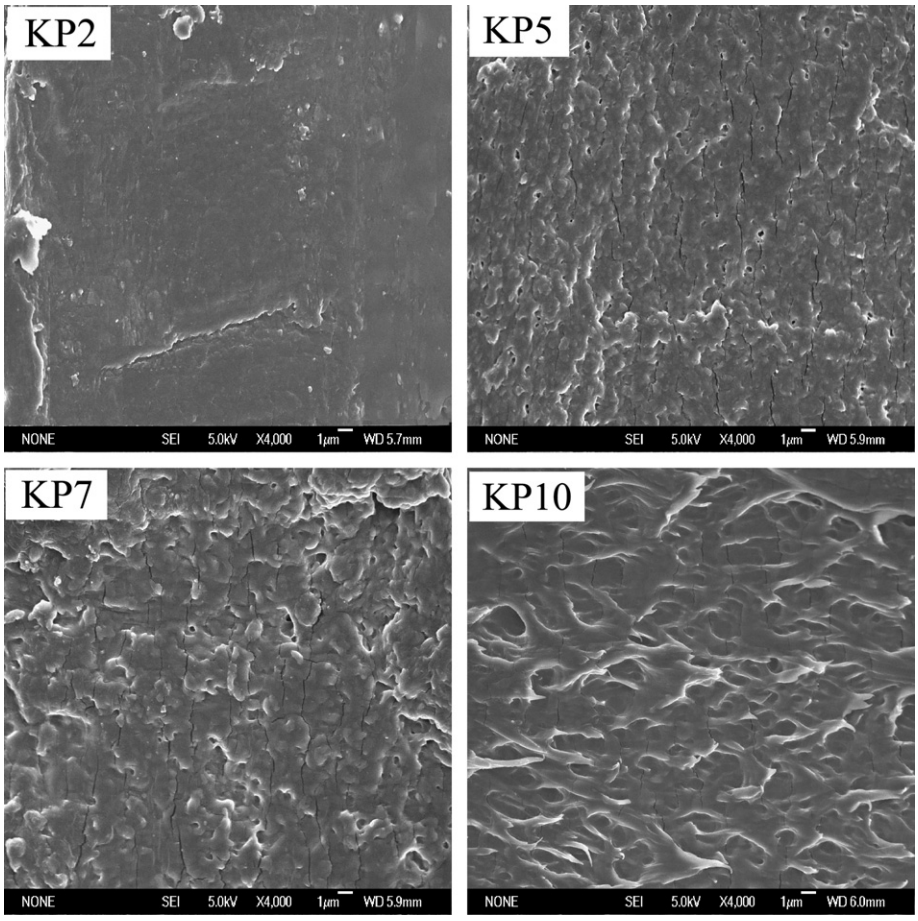


Fig. 5. SEM images of the cross-sections of the KP films.

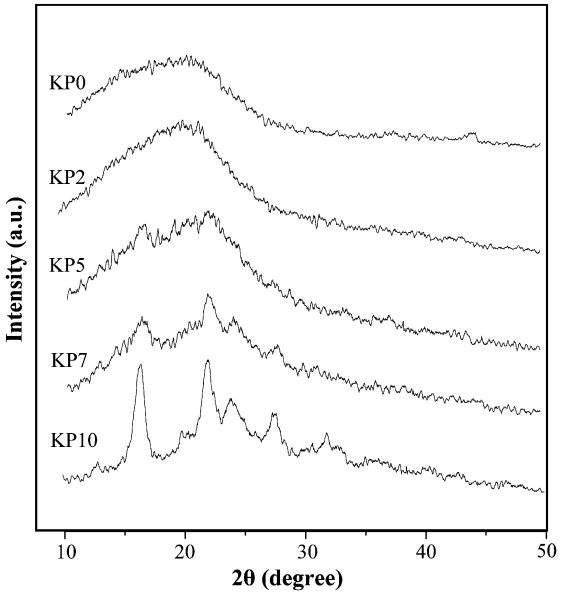


Fig. 6. X-ray diffraction patterns of the KP films.

### 3.4. Infrared spectroscopy of the blend films

IR spectra were used to characterize the structure of the substances and investigate the interaction between the two polymers. Fig. 7 shows the IR spectra of the OH stretching region of the KP membranes. From the IR spectra of KP10, pure PDADMAC, it can be seen that a strong peak at 3440 $cm^{-1}$ corresponded to the stretching and distortion of hydroxyl, owing to the hygroscopic nature of the polymer. The absorption band around 3330 $cm^{-1}$ corresponding to the stretching of hydroxyl for KP0, narrowed and gradually shifted to a high wave number 3407 $cm^{-1}$ and became strong when KGM blended with PDADMAC. It indicated that an intramolecular hydrogen-bonded state of pure KGM was interrupted in the blend films (Liu & Xiao, 2004).

Fig. 8 shows the IR spectra of the membranes in the wavelength region 1800–800 $cm^{-1}$. The peak at 2945, 2830, 1478 and 1385 $cm^{-1}$ assigned to methyl and methylene groups. The band at 1640 $cm^{-1}$ related to the vibration of $NR_4$ (Lin, Zhong, Chen, Zhou, & He, 2003). Under electrostatic interaction, the bond of C—O—C at 1020 $cm^{-1}$ for KP0 shifted to higher wavenumbers in the blend films of KP2, KP5 and KP7. The distortion vibration of methyl at 1478 $cm^{-1}$ for PDADMAC was weakened and gradually shifted to lower wavenumbers with increasing content of KGM in the blend films. At the same time the characteristic absorption bands at 1640 and 958 $cm^{-1}$ in the blend films became weaken

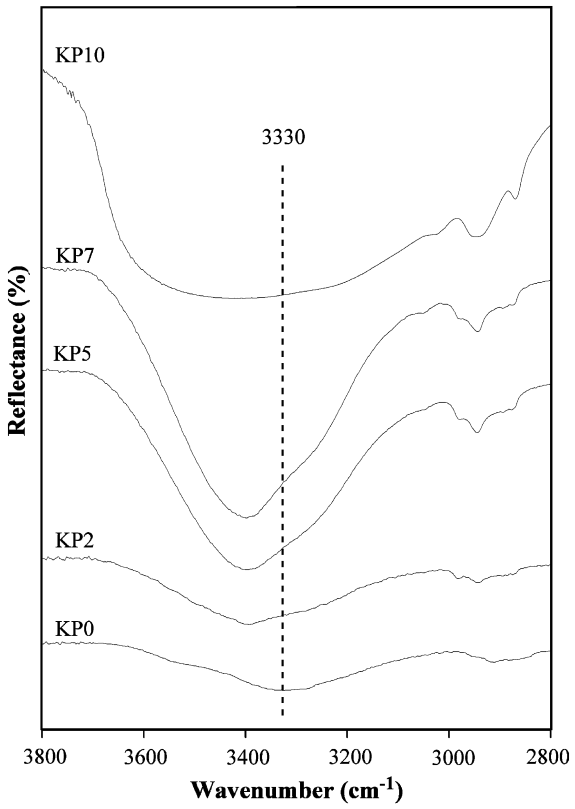


Fig. 7. IR spectra of the KP films in the wavelength region 3800–2800 $cm^{-1}$.

too. These effects were a consequence of the electronic distribution changes in electron distribution in the molecular structure of PDADMAC and KGM, resulted from the strong electrostatic interaction. Furthermore the characteristic absorption bands of mannose in the blend films at 874 and 805 $cm^{-1}$ became weaker with the increasing content of PDADMAC in the blend films, indicating that strong electrostatic interaction exists between KGM and PDADMAC.

### 3.5. Thermal stability

Fig. 9 shows the TG thermograms of the films and the detailed thermo-gravimetric data for the films are displayed in Table 1. All the films had weight loss of about 13% in the range of 50.0–120.0 °C, owning to the release of water molecules from the films. With the increase of the temperature, KGM and PDADMAC began the step of maximum weight loss at 208.1 and 335.0 °C while KP2, KP5 and KP7 shown at 252.3, 235.4 and 223.5 °C respectively. It was found that the onset temperatures of weight loss for the blend films were higher than that of KGM and lower than PDADMAC. It appears that blending with the synthetic polymer could improve the thermo-stability of the natural polymer. It was also found that the onset temperatures for weight loss from the blend films increased with decreasing PDADMAC content, the

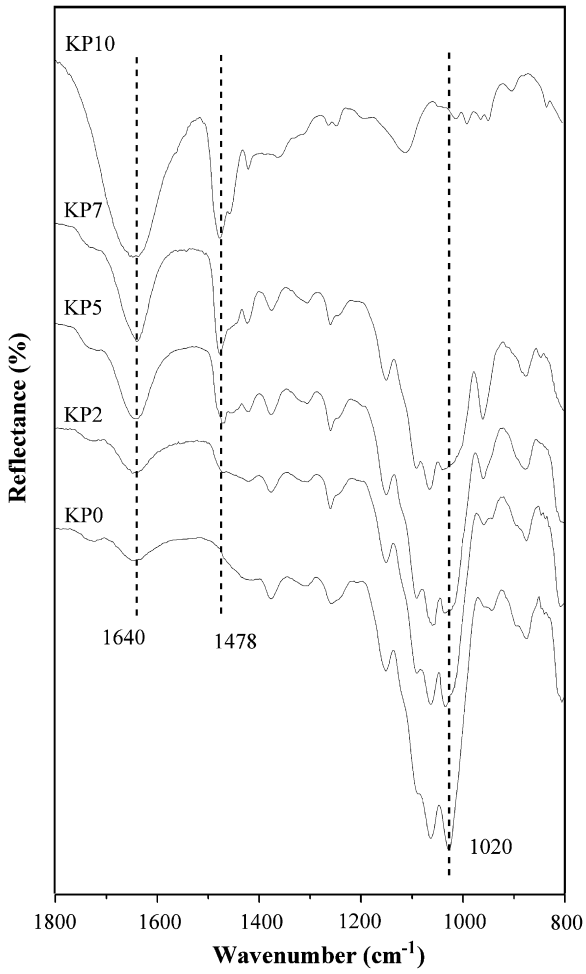


Fig. 8. IR spectra of the KP films in the wavelength region 1800–800 $cm^{-1}$.

order of thermo-stability of the films was KP2, KP5 and KP7. KP2 showing two steps of weight loss similar to that of KP0 while KP5 and KP7 showed three steps similar to that of KP10. The greatest weight loss of the films was attributed to the decomposition of PDADMAC and KGM.

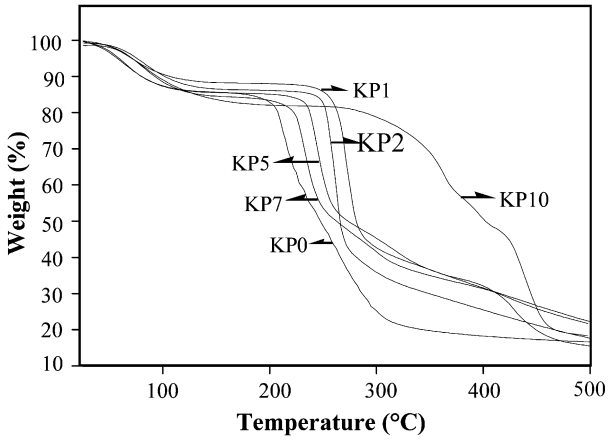


Fig. 9. TG thermograms of the KP films.

Table 1
Thermo-gravimetric data of the KP films

| Sample | Decomposition stage | Temperature range (°C) | Weight loss (%) |
|---|---|---|---|
| KP0 | 1 | 40.5–97.3 | 13.02 |
| | 2 | 208.1–310.0 | 65.34 |
| KP2 | 1 | 60.0–110.8 | 12.43 |
| | 2 | 252.3–270.4 | 55.23 |
| KP5 | 1 | 48.2–102.0 | 13.40 |
| | 2 | 235.4–353.4 | 40.17 |
| | 3 | 412.4–449.6 | 12.72 |
| KP7 | 1 | 59.5–113.5 | 13.95 |
| | 2 | 223.5–333.7 | 47.32 |
| | 3 | 355.1–413.5 | 4.19 |
| KP10 | 1 | 57.0–121.5 | 14.05 |
| | 2 | 335.0–369.5 | 21.21 |
| | 3 | 389.4–403.8 | 5.19 |
| | 4 | 425.2–458.9 | 27.36 |

The DSC curves of the films are displayed in Fig. 10. The curves of all the films showed an endothermic peak at 80.2–104.7 °C, which was attributed to the loss of moisture. The exothermic peak around 228.4 °C for KP0 resulted from the thermal degradation of KGM. The exothermic peak around 305.7 °C for KP10 was attributed to the thermal degradation of PDADMAC. The DSC curves of the films of KP2, KP5 and KP7 showed an exothermic peak at 264.4, 253.7 and 258.6 °C. It can be seen that KP2 has the highest thermo-stability of the blend films, which was caused by the good miscibility. It was found that the DSC curves of KP5, KP7 and KP10 displayed obvious endothermic peaks around 232.3–254.9 °C and the curve of KP2 showed a weak endothermic peak around 251.7 °C, which were attributable to the melting of the crystal phase in the blend films. These results of TG and DSC were in agreement with results of SEM and X-ray.

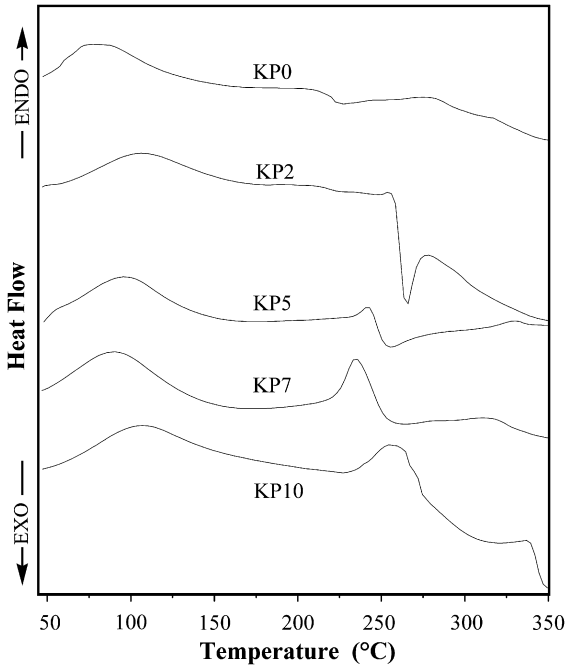


Fig. 10. DSC thermograms of the KP films.

### 3.6. Mechanical properties

Because polymer materials, such as films, may be subjected to various kinds of stress during use, the determination of the mechanical properties involves not only scientific but also technological and practical aspects (Freddi, Romano, Massafra, & Tsukada, 1995).

Fig. 11 shows the effect of the PDADMAC content on the stress-at-break ($\sigma_b$) of the KP blend films. It can be seen that the addition of PDADMAC to KGM was effective in enhancing the mechanical properties films. The strain-at-break of the pure KGM was 67.07 MPa. With the increasing PDADMAC content, the tensile strength of the blends increased and the maximum stress achieved was 106.5 MPa at a PDADMAC content 20 wt%, and then decreased. The large increase in the tensile strength of the KP blend films indicated the presence of intermolecular interactions

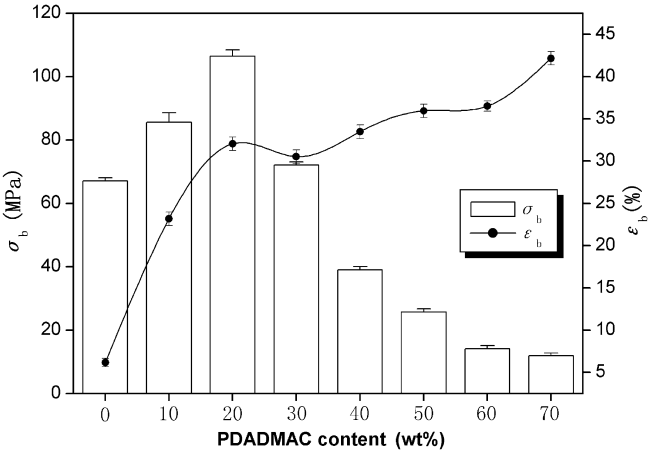


Fig. 11. Dependence of $\sigma_b$ (□) and $\varepsilon_b$ (●) on the PDADMAC content.

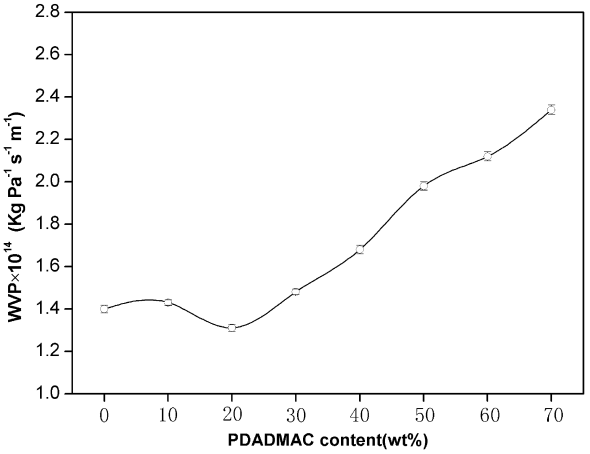


Fig. 12. Dependence of WVA on the PDADMAC content.

Table 2
Antibacterial activities of the films

| Sample | *B. subtilis* ($G^+$) | *S. aureus* ($G^+$) | *E. coli* ($G^-$) | *P. aeruginosa* ($G^-$) | *Saccharomyces* |
|---|---|---|---|---|---|
| KP0 | − | − | − | − | − |
| KP2 | + | + | − | − | − |
| KP5 | + | + | − | − | − |
| KP7 | + | + | − | − | − |
| KP10 | + | + | + | − | − |

+, inhibition; −, no inhibition.

between KGM and PDADMAC. With increasing PDADMAC content, since the intermolecular interactions were not strong enough prevent crystallization of PDADMAC, the tensile strength of the blend films decreased. The results are consistent with the SEM and XRD analysis.

The curve with black dots in Fig. 11 shows the dependence of the strain-at-break ($\varepsilon_b$) on the PDADMAC content for the KP films. The strain-at-break of KGM was 6.17%. When the PDADMAC content was less than 20 wt%, the changes in the elongation at break expressed a tendency similar to that of the tensile strength for the blend films, and also reached the maximum 32.04% when the PDADMAC content was 20 wt%, and then decreased. But when the PDADMAC content was higher than 30 wt%, the elongation at break began to increase slightly with the increase in the PDADMAC content. This was probably because the crystal phase of PDADMAC could be oriented under stress.

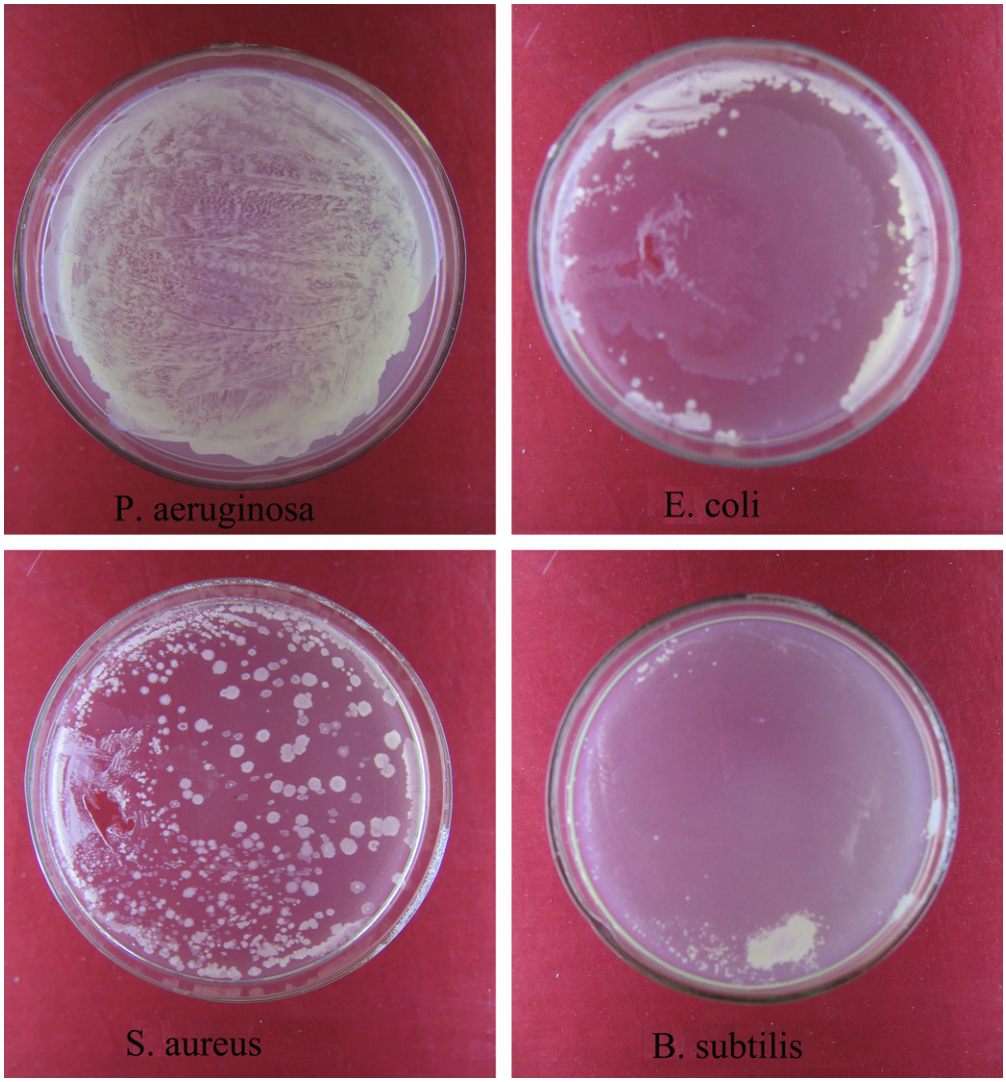


Fig. 13. Effect of PDADMAC on growth of four bacteria.

### 3.7. Water vapor permeability (WVP)

An excessively high RVP gradient can result in altered water vapour permeability values due to the high degree of hydrophilicity and swelling of the structure. By applying a small RVP gradient across the film samples, non-Fickian behaviour of the films would be avoided (Cheng et al., 2002). Fig. 12 shows the effect of the PDADMAC content on WVP of the films. It can be seen that the KP2 film had a lower WVP than other films. It is known that WVP of a film is dependent upon the number of "available" polar (—OH) groups that the polymer possesses. With the incorporation of PDADMAC, the intermolecular interaction occurred between KGM and PDADMAC and diminish the number of available —OH groups, thereby impeding diffusion of water vapour. With the increase of the PDADMAC content, the enhancement of WVP may be due to the strong hydrophilic nature of PDADMAC.

### 3.8. Antibacterial assessments

Our work was aimed at finding a novel antibacterial biomacromolecular material, so the antibacterial activity of the films against *S. aureus*, *B. subtilis*, *E. coli*, *P. aeruginosa*, and *Saccharomyces* were measured by the halo zone test and the double plate method.

The ability of the films to inhibit growth of the tested strains are listed in Table 2. The results obtained by the halo zone test revealed that KGM had no antibacterial activity at all while KP10 had antibacterial activity against *S. aureus*, *B. subtilis* and *E. coli*, but not against *P. aeruginosa*, and *Saccharomyces*. As for the blend films, they had inhibitory effect against *B. subtilis* and *S. aureus* which are Gram-positive bacteria ($G^+$) but no against *E. coli* and *P. aeruginosa* which are Gram-negative bacteria ($G^-$) and Saccharomyces.

The results obtained by the double plate method for KP10 are shown in Fig. 13. The inhibitory zone of the bacteria was transparent and the growth zone was opaque. It can be seen that the entire zone was transparent for *B. subtilis*; most of the zone were transparent but some opaque regions were seen for *S. aureus* and *E. coli*; the whole zone was opaque for *P. aeruginosa*. So it was predicted that *B. subtilis* was more susceptible to KP10 than *S. aureus* and *E. coli*. Interestingly the film blends had no activity against *E. coli* while pure PDADMAC had. This may be explained if the antibacterial activity of the blend films depended on the efficient concentration of the antibacterial substance, the quaternary ammonium groups.

Fig. 14 shows the dependence of the antibacterial activity of the KP film against *B. subtilis* on the PDADMA content. It was found that there was no inhibition zone for the control and KGM; but a clear inhibition zone was observed for the film blends. However, the size of the inhibition zone decreased a reduction in the PDADMAC content in the blends. Therefore it was predicted that the antibacterial activity of the blends might be associated with the concentration of PDADMAC. The antibacterial mechanism of the blends may be interpreted as follows: adsorption onto the bacterial cell surfaces, binding to the cytoplasmic membrane, disruption of membrane and subsequent leakage of K+ ions and other cytoplasmic constituents (Tashiro, 2001). All the processes should be facilitated by electrostatic interaction. So the blends carrying higher charge density had higher antibacterial activities.

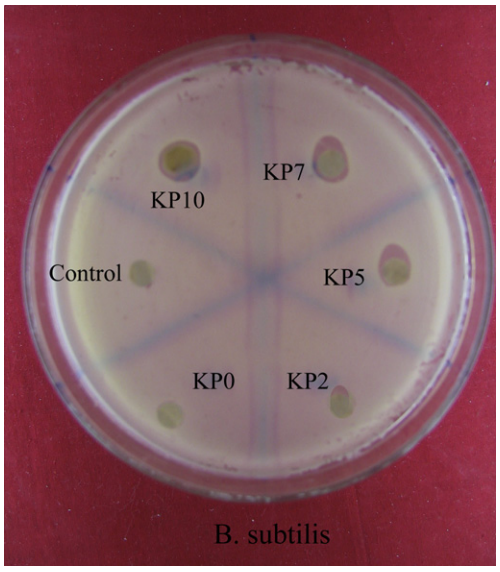


Fig. 14. Dependence of the antibacterial activity on the PDADMA content.

## 4. Conclusions

A novel antibacterial film was prepared by blending KGM and PDADMAC in aqueous systems. The films exhibited excellent antibacterial activity against *B. subtilis* and *S. aureus* but not against *E. coli*, *P. aeruginosa* and *Saccharomyces*. The results of the density determination, SEM and XRD predicted that there was good miscibility between KGM and PDADMAC in the blends when the PDADMAC content was less than 70 wt% and the highest miscibility appeared when the PDADMAC content was 20 wt%. ATR-IR showed that strong intermolecular hydrogen bonds electrostatic interaction occurred between the negative charge groups of KGM and the quaternary ammonium groups of PDADMAC in the blends. The tensile strength and the elongation and break of the blends were improved largely to 106.5 MPa and 32.04% and the water vapour permeability decreased when the PDADMAC content was 20 wt%. The thermal stability of the blends was higher than the natural polymer. From the work, we predict that the blend film KP2 had the properties as antibacterial materials and has potential applications in the biomedical field.

## Acknowledgments

This work was supported by the fund from the Education Office of Hubei Province, Peoples Republic of China (D200625004).

## References

Alonso-Sande, M., Cuna, M., & Remunan-Lopez, C. (2006). Formation of new glucomannan–chitosan nanoparticles and study of their ability to associate and deliver proteins. *Macromolecules, 39*(12), 4152–4158.

Alvarez-Mancenido, F., Braeckmans, K., De Smedt, S. C., Demeester, J., Landin, M., & Martinez- Pacheco, R. (2006). Characterization of diffusion of macromolecules in konjac glucomannan solutions and gels by fluorescence recovery after photo bleaching technique. *International Journal of Pharmaceutics, 316*(1-2), 37–46.

Begin, A., & Van Calsteren, M. R. (1999). Antimicrobial films produced from chitosan. *International Journal of Biological Macromolecules, 26*(1), 63–67.

Chen, L. G., Liu, Z. L., & Zhuo, R. X. (2005). Synthesis and properties of degradable hydrogels of konjac glucomannan grafted acrylic acid for colon-specific drug delivery. *Polymer, 46*(16), 6274–6281.

Cheng, L. H., Abd Karim, A., Norziah, M. H., & Seow, C. C. (2002). Modification of the microstructural and physical properties of konjac glucomannan-based films by alkali and sodium carboxymethylcellulose. *Food Research International, 35*, 829–836.

Chun, S. Y., Kim, H. I., & Yoo, B. (2006). Effect of gum addition on the rheological properties of rice flour dispersions. *Food Science and Biotechnology, 15*(4), 589–594.

Coma, V., Martial-Gros, A., Garreau, S., Copinet, A., Salin, F., & Deschamps, A. (2002). Edible antimicrobial films based on chitosan matrix. *Journal of Food Science, 67*(3), 1162–1169.

Cooksey, K. (2005). Effectiveness of antimicrobial food packaging materials. *Food Additives and Contaminants, 22*(10), 980–987.

Cuna, M., Alonso-Sande, M., Remunan-Lopez, G., Pivel, J. P., Alonso-Lebrero, J. L., & Alonso, M. J. (2006). Development of phosphorylated glucomannan-coated chitosan nanoparticles as nanocarriers for protein delivery. *Journal of nanoscience and nanotechnology, 6*(9-10), 2887–2895.

Freddi, G., Romano, M., Massafra, M. R., & Tsukada, M. (1995). Silk fibroin/cellulose blend films: Preparation, structure, and physical properties. *Journal of Applied Polymer Science, 56*, 1537–1545.

Kim, S. C., Klempner, D., & Frisch, H. L. (1976). Polyurethane interpenetrating polymer networks. I. Synthesis and morphology of polyurethane-poly(methyl methacrylate) interpenetrating polymer networks. *Macromolecules, 9*(2), 258–263.

Kirker, K. R., & Prestwich, G. D. (2004). Physical properties of glycosaminoglycan hydrogels. *Journal of Polymer Science: Part B: Polymer Physics, 42*(23), 4344–4356.

Li, B., Peng, J. L., Yie, X., & Xie, B. J. (2006). Enhancing physical properties and antimicrobial activity of konjac glucomannan edible films by incorporating chitosan and nisin. *Journal of Food Science, 71*(3), C174–C178.

Li, B., Kennedy, J. F., Peng, J. L., Yie, X., & Xie, B. J. (2006). Preparation and performance evaluation of glucomannan–chitosan–nisin ternary antimicrobial blend film. *Carbohydrate Polymers, 65*(4), 488–494.

Lin, X. J., Zhong, A. Y., Chen, D. B., Zhou, Z. H., & He, B. B. (2003). Studies on self-assembly and characterization of polyelectrolytes and organic dyes. *Journal of Applied Polymer Science, 87*, 369–374.

Liu, C. H., & Xiao, C. B. (2004). Characterization of konjac glucomannan–quaternized Poly (4-vinyl-*N*-butyl) pyridine blend films and their preservation effect. *Journal of Applied Polymer Science, 93*, 1868–1875.

MollLler, H., Grelier, S., Pardon, P., & Coma, V. (2004). Antimicrobial and Physicochemical Properties of chitosan-HPMC-based films. *Journal of Agricultural and Food Chemistry, 52*(21), 6585–6591.

Nishinari, K., Williams, P. A., & Phillips, G. O. (1992). Review of the physico-chemical characteristics and properties of konjac mannan. *Food Hydrocolloids, 6*, 199–222.

Tashiro, T. (2001). Antibacterial and bacterium adsorbing macromolecules. *Macromolecular Materials and Engineering, 286*(2), 63–87.

Wandrey, C., Hernandez-Barajas, J., & Hunkeler, D. (1999). Diallyldimethylammonium chloride and its polymers. *Advances in Polymer Science, 145*, 123–182.

Wandrey, C., Jaeger, W., & Reinisch, G. (1982). Determination of the relative molecular weight of poly(dimethyldiallylammonium chloride) by viscosimetry of solutions. *Acta Polymerica, 33*(2), 156–158.

Xiao, C. B., Lu, Y. S., Gao, S. J., & Zhang, L. N. (2001). Characterization of konjac glucomannan–gelatin blend films. *Journal of Applied Polymer Science, 79*(9), 1596–1602.

Xiao, C. B., Gao, S. J., Wang, H., & Zhang, L. N. (2000). Blend films from chitosan and konjac glucomannan solutions. *Journal of Applied Polymer Science, 76*(4), 509–515.

Yang, G., Zhang, L., & Feng, H. (1999). Role of polyethylene glycol in formation and structure of regenerated cellulose microporous membrane. *Journal of Membrane Science, 161*, 31–40.

Yang, X. J., Wang, X., Wang, H., Zhu, J., Lu, L., Zhou, T., & Lian, J. (2003). Preparation and characterization of poly(dimethyldiallyl ammonium) chloride and antiglobulin tests for antibody detection. *Journal of Applied Polymer Science, 87*, 1957–1961.

Yu, H. Q., Huang, A., & Xiao, C. B. (2006). Characteristics of konjac glucomannan and poly(acrylic acid) blend films for controlled drug release. *Journal of Applied Polymer Science, 100*(2), 1561–1570.